in position of the fluid velocity, which is the coefficient $\alpha f(t)$ in term (a) (Eq. 1).

For brevity we omit initial and boundary conditions necessary for a complete statement of model. Suffice it to indicate, however, that the degree of separation depends not only on the coupled actions expressed in Eqs. 1–3, but also, in the case of the total reflux operation here described, on the total solute content of the system, such content depending on initial conditions.

Dependent variables in the conservation, rate, and equilibrium equations are identified as ϕ_f, ϕ^*_f, and ϕ_s, being, respectively, the dimensionless fluid composition, fluid composition in equilibrium with the adsorbent phase, and the adsorbent-phase composition. Independent variables are the dimensionless time, t, axial position, z, and system temperature, θ.

The terms in Eqs. 1 and 2 express mass conservation contributions attributable to these mechanisms: (a) axial convection, (b) interstitial, fluid-phase transient, (c) adsorptive-phase transient, (d) axial fluid-phase diffusive loss, (e) lumped-parameter interphase diffusive-transport rate.

Parametric action resides in bringing into synchronism and into suitable phase-angle relation the alternating flow velocity in (a), $\alpha f(t)$, with the periodically cycling temperature θ in (g); the effect of this action penetrates the system of equations successively through the terms (f), (e), and (c).

The magnitude of separation by means of "parapumping" depends on the numerical values of the equation coefficients α, κ, η, λ, the function ϕ^*_f [ ], and the balance among them. These experimental results and others (*4, 5*) serve to demonstrate that the parametric-pumping principle applied to separation is indeed an operable one, and that the system coefficients are physically attainable in workable combinations. Coefficients are identified thus: α, velocity amplitude; κ, ratio of volume of adsorptive phase to that of the interstitial fluid phase; η, dissipative axial diffusivity of solute;

$$\lambda = (D/R^2)(1/\omega)$$

that is, reciprocal characteristic diffusion time D/R^2 relative to the frequency ω of the axial fluid convective displacements. (Term D is a lumped interphase-diffusion constant, and R is the adsorbent-particle radius.) The properties of the adsorptive equilibrium function ϕ^*_f [ ] complete identification of the essential parameters.

We have found the dimensionless rate constant λ to be particularly important, as shown by the ordering of separation results (Fig. 2) according to experimental frequency. Figure 2 also shows that numerical, computer solutions of the equations predict properly the *qualitative* dependence of separation on λ, the development of limiting separations, and the effect of elapsed time. The equations served a priori to predict that large separations were likely, and thereby provided the incentive for performance of these experiments. *Quantitative* matching of the mathematical model with experiment will involve secondary but important factors such as temperature-dependence of system coefficients, detailed thermal responses within the column, and strategy of computation.

Figure 3 presents composition profiles, computed through Eqs. 1 and 2, based on experimental equilibrium values for the toluene-heptane-silica gel system (*6*). The steep wave front after downflow is that of an adsorption wave, and its shape reflects the effect of the nonlinear, Langmuir-type adsorption isotherm; characteristically of such systems the desorption (upflow) wave is relatively diffuse, as shown. The direction of the interphase-diffusion gradient ($\phi^*_f - \phi_f$) is noted to alternate during each cycle. Parametric action serves to build up, through successive adsorption-desorption steps, a steep solid-fluid adsorption wave that constitutes an effective barrier to the passage of fluid-phase solute through the bottom end of the column. With a 180-deg phase shift between temperature and flow variables, the solute barrier is predicted to appear at the top of the column.

Earlier reports about parametric pumping concern the recuperative mode (*4*), in which heat recovery is an intimate part of the system, and a suggestion (*5*) that parametric-pumping separation may serve as a candidate model for active transport through membranes in biological cells, the intensive thermodynamic variable in this instance being *p*H instead of temperature.

RICHARD H. WILHELM
NORMAN H. SWEED
Department of Chemical Engineering,
Princeton University,
Princeton, New Jersey 08540

References and Notes

1. Matheson, Coleman, and Bell.
2. Harvard Apparatus Co.
3. Cary-14 recording spectrophotometer; 2685-Å wavelength.
4. R. H. Wilhelm, A. W. Rice, A. R. Bendelius, *Ind. Eng. Chem. Fundamentals* **5**, 141 (1966).
5. R. H. Wilhelm, in *Intracellular Transport*, K. B. Warren, Ed. (Academic Press, New York, 1966), p. 199.
6. G. S. Robins performed the equilibrium measurements that were employed in these theoretical calculations.
7. Supported by NSF grant GK-1427X. Computations were by the Princeton University Computer Center, which was aided by NSF grant GP-579. One of us (N.H.S.) holds an NSF graduate fellowship. We thank R. W. Rolke for helpful discussions.

17 November 1967

■

Kornerupine: Its Crystal Structure

Abstract. *Three-dimensional analysis of the crystal structure of kornerupine reveals the crystallochemical formula* $Mg^{VI}_2Mg^{VI}Al^{VI}_6[Si_2O_7]$ $[(Al,Si)_2SiO_{10}]O_4(OH)$, *with four formula units in the structure cell of* a = *16.100 (2) Å,* b = *13.767(2) Å,* c = *6.735(2) Å; space group,* Cmcm. *The unusual crystal structure includes walls of Al-O edge- and corner-sharing octahedra, and chains of alternating Mg-O and Al-O octahedra fused to the walls by further edge-sharing to form dense slabs. These slabs are held together by* $[Si_2O_7]$ *corner-sharing tetrahedral pairs and* $[(Al,Si)_2SiO_{10}]$ *corner-sharing tetrahedral triplets.*

The curious mineral kornerupine was named, and described from its type locality in Fiskenaesset, Greenland, by Lorenzen (*1*) after the Danish geologist A. Kornerup. Many other occurrences have since been recorded. The most detailed account of the crystal chemistry of kornerupine, including references to its paragenesis, is by McKie (*2*).

The chemistry of kornerupine has had a tumultuous history which is not surprising in view of its complex crystal structure. Mineralogy texts usually present its formula as $MgAl_2SiO_6$, but recent detailed work by McKie on material from Mautia Hill, Tanganyika, led him to propose the empirical formula $Na_{0.01}Ti_{0.02}Mg_{3.69}Fe^{3+}_{0.37}Al_{6.36}Si_{3.71}B_{0.41}O_{21.75}(OH)_{0.25}$, with four such formulas in the structure cell. Unambiguous interpretation of this formidable composition requires careful analysis of the crystal structure, which was undertaken on an eminently suitable crystal from Mautia Hill (*3*).

The structure cell of kornerupine (Table 1) suggested that the most propitious axis of rotation was *c*[001]. Ten levels of three-dimensional data to $2\theta = 70°$ were collected with a Pailred automatic diffractometer using

Table 1. Structure-cell data for kornerupine (*2*).

a(Å)	b(Å)	c(Å)	Space group	Formula	Z	Density (obs.)
16.100	13.767	6.735	*Cmcm*	$Mg_3Al_6(Si,Al)_5O_{21}(OH)$	4	3.29_7

Table 2. Atom coordinates for kornerupine

Atom	Multiplier	x	y	z	B(Å^{-2})
Mg(1)	1.84	0.1226(2)	0.1402(3)	¼	0.75(5)
Mg(2)	1.0	½	.1464(5)	¼	.71(7)
Si(1)	2.2	0.4018(2)	.3530(2)	¼	.12(3)
Si(2)	1.0	0	.3425(4)	¼	.33(6)
(Al,Si)(1)	2.0	0.1794(2)	.3330(2)	¼	.15(4)
Al(2)	2.0	.2147(2)	0	0	.42(3)*
Al(3)	2.0	.3146(2)	0.1407(2)	¼	.30(3)
Al(4)	2.0	.0928(2)	½	0	.40(3)*
O(1)	2.0	.2242(6)	0.0439(6)	¼	.81(10)
O(2)	2.0	.4032(6)	.0457(5)	¼	.42(9)
O(3)	2.0	.4032(6)	.2354(6)	¼	.68(9)
O(4)	4.0	.1381(6)	.1008(7)	−0.0520(9)	.62(6)
O(5)	2.0	.2346(6)	.2356(7)	¼	1.27(12)
O(6)	4.0	.3162(4)	.0942(4)	−0.0448(9)	0.64(6)
O(7)	2.0	.0842(6)	.2794(6)	¼	.77(10)
O(8)	2.0	.5000	.0878(6)	−0.0505(13)	.57(8)
O(9)	1.0	.5000	.3875(11)	¼	1.53(18)
O(10) = (OH)	1.0	0	.0882(10)	¼	1.32(17)

* After equal distribution of Fe^{3+} over these sites.

monochromatized MoK_α radiation (*4*). Altogether 1549 independent intensities were available after averaging of symmetry-equivalent spectra; 1047 of them were of "nonzero" intensity. These data were then processed in a straightforward manner to obtain $|F_{obs}|$. No transmission-factor correction was applied because of the favorable shape and relatively low density of the mineral.

The data were then read into an IBM-7094 computer employing the program MAGIC (*5*), which assigns phases by the symbolic addition procedure (*6*). This program requires only a minimum of information, including cell type and dimensions, the total number of each atomic species in the cell, and their corresponding scattering-factor tables. Sixteen of the 18 atoms in the asymmetric unit were unambiguously revealed on one of the four combinations afforded by the computation, which took only 4 minutes of computer time. Two cycles of least-squares coordinate refinement gave $R_{hkl} = 0.26$, whereupon the remaining two oxygen atoms were located on a subsequent three-dimensional electron-density map. Full-matrix least-squares refinement converged to $R_{hkl} = 0.113$. Final coordinates, multipliers, and isotropic temperature factors are presented in Table 2.

The crystal structure of kornerupine is quite complicated (Fig. 1). Two sets of coordinate-independent Al-O octahedra link, by way of corner- and edge-sharing, to form planar octahedral walls that run parallel c[001] (Fig. 1a). Chains of alternating Mg-O and Al-O edge- and corner-sharing octahedra run parallel a[100] (Fig. 1b) and link to the Al-O octahedral walls by edge-sharing. Thus the walls and the chains constitute dense slabs that

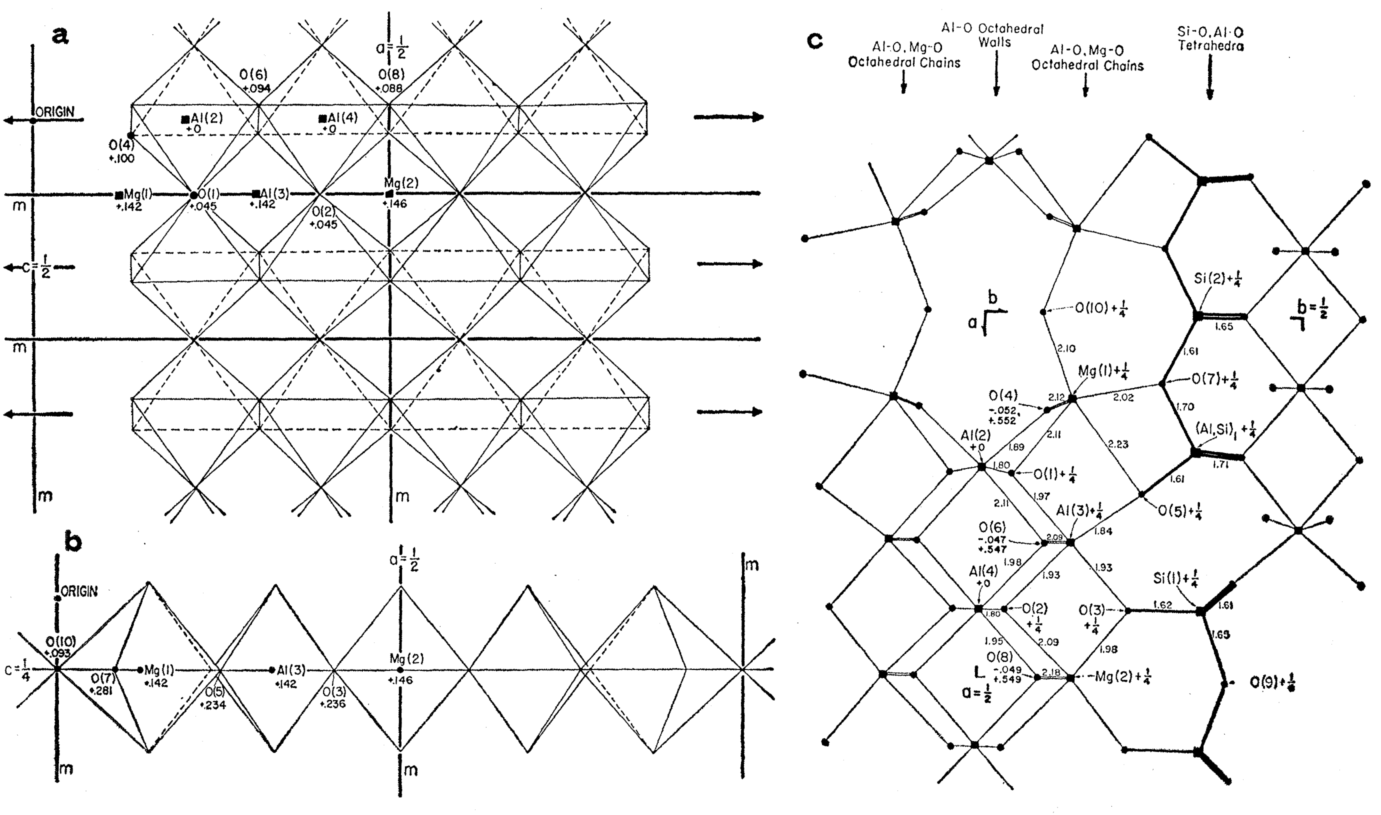

Fig. 1. (a) Octahedral Al-O walls in the crystal structure of kornerupine. The symmetry elements are included; *m* locates the mirror planes and arrows locate the twofold rotors. Heights along *b* are given in fractional coordinates. (b) Chains of alternating Mg-O and Al-O octahedra in kornerupine; they fit above and below the walls in Fig. 1a by edge-sharing. (c) Spoke diagram of the kornerupine crystal structure down *c*[001]. The tetrahedral units are drawn bold; interatomic metal-oxygen distances are included.

are oriented parallel $b\{010\}$. These slabs are in turn joined along $b[010]$ by two kinds of independent tetrahedral units: $[Si_2O_7]$ corner-sharing pairs and $[(Al,Si)_2SiO_{10}]$ corner-sharing triplets (Fig. 1c). The interesting T_3O_{10} triplets are not new to science, being recently reported (*7*) in the crystal structure of ardennite; as in the ardennite structure, they utilize a mirror plane. The full kornerupine structure is a stable three-dimensional arrangement. Although apparently there are no limitingly close-packed layers of oxygen atoms, the structure evidently conserves space efficiently, since the volume per oxygen atom is 17.0 $Å^3$.

Metal-oxygen distances appear in Fig. 1c: Al-O octahedral distances average 1.91, 1.93, and 1.97 Å; Mg-O octahedra, 2.09 and 2.12 Å; Si-O tetrahedra, 1.62 and 1.63 Å; and (Al, Si)-O tetrahedra, 1.68 Å, with metal-oxygen distances ± 0.02 Å. The Mg(1)-O octahedron is highly distorted and must be considered separately in the crystallochemical formula. These Mg(1)-O octahedra join by reflection across $a\{100\}$ by way of hydroxyl (OH) groups. The crystallochemical formula is written

$$Mg^{VI}{}_2Mg^{VI}Al^{VI}{}_6[Si_2O_7][(Al,Si)_2SiO_{10}]O_4(OH)$$

of which there are four units in the structure cell. The multipliers and temperature factors assist in locating the minor-element substitutions. McKie's formula may be written

$$(Mg, Na)_2\,Mg\,(Al, Fe, Mg)_6\,[Si_2O_7]\\ [(Al, Si)_2\,(Si, B)O_{10}]\,O_4\,(O, OH).$$

We present electrostatic valence-bond strengths in Table 3, computed according to Pauling (*8*). Deviations from saturation are slight, confirming the assignment of the metals on the basis of their interatomic distances. It is seen that O(10) must be a hydroxyl group; it accounts for the presence of water in the wet-chemical analyses reported for kornerupine.

Table 3. Electrostatic valence-bond strengths (ξ) in kornerupine.

Atom	Associated metals	ξ
O(1)	Al(3) + Mg(1) + Al(2) + Al(2′)	1.8
O(2)	Al(3) + Mg(2) + Al(4) + Al(4′)	1.8
O(3)	Si(1) + Al(3) + Mg(2)	1.8
O(4)	Si(1) + Mg(1) + Al(2) + Al(2′)	2.3
O(5)	(Al,Si)(1) + Mg(1) + Al(3)	1.7
O(6)	(Al,Si)(1) + Al(2) + Al(4)	1.9
O(7)	Si(2) + (Al,Si)(1) + Mg(1)	2.2
O(8)	Si(2) + Al(4) + Al(4′) + Mg(2)	2.1
O(9)	Si(1) + Si(1′)	2.0
O(10) = (OH)	Mg(1) + Mg(1′)	0.7

PAUL B. MOORE
J. MICHAEL BENNETT
Department of the Geophysical Sciences, University of Chicago, Chicago, Illinois 60637

References and Notes

1. J. Lorenzen, *Medd. Groenland* **7**, 19 (1884).
2. D. McKie, *Mineral. Mag.* **34**, 346 (1965).
3. Crystals supplied by D. McKie.
4. We thank J. V. Smith for help.
5. E. B. Fleisher, R. B. K. Dewar, A. L. Stone, in *Amer. Cryst. Assoc. Winter Meeting Progr. Abstr.* (1967), p. 20. We thank R. B. K. Dewar and S. Hawkinson for assistance in setting up this program.
6. J. Karle and I. L. Karle, *Acta Cryst.* **21**, 849 (1966) (a good introduction).
7. G. Donnay and R. Allmann, in *Amer. Cryst. Assoc. Summer Meeting Progr. Abstr.* (1967), p. 91.
8. L. Pauling, *The Nature of the Chemical Bond* (Cornell Univ. Press, Ithaca, N.Y., ed. 3, 1960), p. 547.
9. Supported by NSF grant GA 907 to P.B.M. and by Petroleum Research Fund grant 642-A2 to J.M.B. by American Chemical Society.

26 October 1967

Ten-Armed Fossil Cephalopod from the Pennsylvanian of Illinois

Abstract. Jeletzkya douglassae *Johnson and Richardson is described as the oldest known representative of an extant squid group. The species is known from a single specimen from the Middle Pennsylvanian of Illinois. This very unusual fossil consists of the complete tentacular crown and a fragile shell. The arms bear hooks in double rows.*

A new locality in the Mazon Creek area of northeastern Illinois is yielding an extensive and almost wholly undescribed fossil fauna consisting largely of soft-bodied marine animals (*1*). The fossils occur in ironstone concretions in the Middle Pennsylvanian Francis Creek shale. The fauna includes a variety of polychaete annelids, mollusks, crustaceans, jellyfish, and several animals of uncertain zoological affinities (*2*). Recently a member of the Earth Science Club of Northern Illinois collected a remarkable fossil decapod mollusk from this locality.

The specimen is preserved in a small ironstone concretion 61 by 52 mm in size. Part of the fossil is revealed on a plane of the concretion split open by the collector. The exposed portion consists of a crown of ten arms; a thin flat shell has been revealed by radiographs. Inasmuch as the ordinal position of this animal is uncertain, we have avoided designating the fossil by a name that might imply a particular zoological affinity (*3*).

Phylum Mollusca
Class Cephalopoda

Jeletzkya Johnson and Richardson, new genus

Type: *Jeletzkya douglassae* Johnson and Richardson, new species. As there is but a single specimen known, the characterization of the genus must be the same as that of the species.

Jeletzkya douglassae Johnson and Richardson, new species

Diagnosis: Decapod with a narrow, nearly flat shell lacking a chambered phragmocone but possessing a short conus. Shell simple, not differentiated into median field and wings. Arms of nearly equal length, provided with paired rows of arm hooks. Holotype and only known specimen, both halves of an ironstone concretion, number 565, in the collection of David Douglass, Western Springs, Illinois.

The tentacular crown of the only specimen known is 30 mm in diameter (see cover). The arms range from 9.5 to 10.5 mm in length and are 2.0 to 2.5 mm wide at their bases; maximum spread of the arms is 30 mm. Strewn along the arms are minute hooks (Fig. 1). Most of the arm hooks are displaced, but on several arms the position shows that they were originally in two rows (Fig. 2). There is no evidence of suckers. In the center of the tentacular crown is an oval, black, nearly flat area. The surface of this unknown structure is organic in appearance. One of our colleagues has suggested that it might be a relic of an ink sac. There is no evidence of jaws or a radula in either half of the concretion.

The shell (Figs. 3 and 4) is concealed within the concretion except where it was intersected on grinding down the outer surface of the concretion. The very small amount of shell material exposed shows that it is extremely thin and fragile. We decided not to prepare out the shell because of the danger of damaging it and the remainder of the fossil; instead we have studied it by single and stereo radiographs (*4*). The shell is about 23.5 mm in length and has a maximum width of 8.0 mm. A millimeter or so of the posterior tip of the shell was removed in grinding down the concretion for x-ray examination. The lateral and stereo radiographs show the shell to